

Accessing weak neutral-current coupling g_{AA}^{eq} using positron and electron beams at Jefferson Lab

Xiaochao Zheng^{a,1}, Jens Erler^{b,2}♣, Qishan Liu^{c,2}♣, Hubert Spiesberger^{d,2}♣

¹Department of Physics, University of Virginia, 382 McCormick Rd, Charlottesville, VA 22904, USA

²PRISMA⁺ Cluster of Excellence, Institute for Nuclear Physics♣ and Institute of Physics♣,
Johannes Gutenberg-University, 55099 Mainz, Germany

Received: date / Accepted: date

Abstract Low-energy neutral-current couplings arising in the Standard Model of electroweak interactions can be constrained in lepton scattering off hydrogen or a nuclear fixed target. Recent polarized electron scattering experiments at Jefferson Lab (JLab) have improved the precision in the parity-violating types of effective couplings. On the other hand, the only known way to access the parity-conserving counterparts is to compare scattering cross sections between a lepton and an anti-lepton beam. We review the current knowledge of both types of couplings and how to constrain them. We also present exploratory calculations for a possible measurement of g_{AA}^{eq} using the planned SoLID spectrometer combined with a possible positron beam at JLab.

Weak Neutral-Current Couplings from Charged Lepton Scattering

The Lagrangian of the weak neutral-current interaction relevant to electron deep inelastic scattering (DIS) off quarks inside the nucleon is given by [1],

$$L_{NC}^{eq} = \frac{G_F}{\sqrt{2}} \sum_q [g_{VV}^{eq} \bar{e} \gamma^\mu e \bar{q} \gamma_\mu q + g_{AV}^{eq} \bar{e} \gamma^\mu \gamma_5 e \bar{q} \gamma_\mu q + g_{VA}^{eq} \bar{e} \gamma^\mu e \bar{q} \gamma_\mu \gamma_5 q + g_{AA}^{eq} \bar{e} \gamma^\mu \gamma_5 e \bar{q} \gamma_\mu \gamma_5 q], \quad (1)$$

where G_F is the Fermi constant. The g_{VV}^{eq} terms are shown here for completeness, even though they are not usually included in equations like (1) as their effects are completely overwhelmed by those of QED, at the very least at lower energies. At lowest order (tree level) in

the Standard Model (SM), the four-fermion couplings are products of the lepton and quark couplings $g_{V,A}^f$ to the Z_0 boson,

$$g_{AV}^{eu} = 2g_A^e g_V^u = -\frac{1}{2} + \frac{4}{3} \sin^2 \theta_W, \quad (2)$$

$$g_{AV}^{ed} = 2g_A^e g_V^d = +\frac{1}{2} - \frac{2}{3} \sin^2 \theta_W, \quad (3)$$

$$g_{VA}^{eu} = 2g_V^e g_A^u = -\frac{1}{2} + 2 \sin^2 \theta_W = -g_{VA}^{ed} = -2g_V^e g_A^d \quad (4)$$

$$g_{AA}^{eu} = -2g_A^e g_A^u = +\frac{1}{2} = -g_{AA}^{ed} = 2g_A^e g_A^d, \quad (5)$$

where θ_W is the weak mixing angle. The couplings g_{AV}^{eq} , g_{VA}^{eq} , and g_{AA}^{eq} [2] agree to lowest order with the widely used quantities C_{1q} , C_{2q} , and C_{3q} , respectively, but are defined independently of the processes in which they are measured. Their precise numerical values differ from those of $C_{1,2,3}$'s because they absorb some higher-order radiative corrections and can also be modified by possible physics beyond the SM.

The g_{AV}^{eq} and g_{VA}^{eq} terms in Eq. (1) induce parity violation and a cross section asymmetry between left- and right-handed electrons scattering off unpolarized protons and nuclei [3]. Specifically, the couplings g_{AV}^{eq} have been measured in elastic scattering, while the combination $2g_{VA}^{eu} - g_{VA}^{ed}$ enters the polarization asymmetry in deep-inelastic scattering (DIS). The coupling g_{AV}^{eq} was also determined in atomic parity violation experiments. The terms involving the g_{AA}^{eq} do not violate parity, but can be accessed by comparing cross sections of lepton to anti-lepton DIS, as we will discuss here.

The parity-violating couplings can be determined in global fits. Figure 1 presents $g_{AV}^{eu} + 2g_{AV}^{ed}$ and similarly Fig. 2 shows $2g_{VA}^{eu} - g_{VA}^{ed}$, in both cases as functions of the combination $2g_{AV}^{eu} - g_{AV}^{ed}$. The constraints in Fig. 1 are strongly dominated by measurements of atomic parity violation in ^{133}Cs [4, 5] and parity-violating electron

^ae-mail: xiaochao@jlab.org

^be-mail: erler@uni-mainz.de

^ce-mail: qisliu@students.uni-mainz.de

^de-mail: spiesber@uni-mainz.de

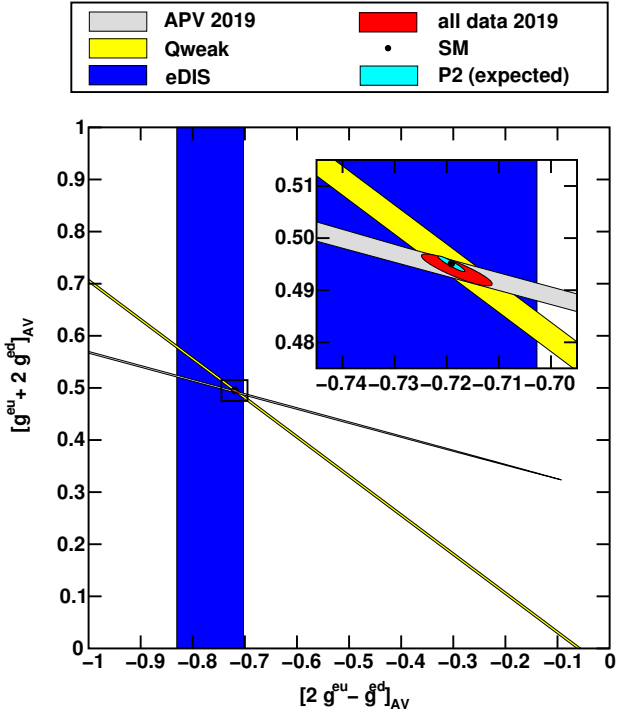


Fig. 1 Current experimental knowledge of the couplings g_{AV}^{eq} . The latest measurement is from the 6 GeV Qweak experiment [7] at JLab. The Atomic Parity Violation ("APV 2019") results shown utilized the theory calculations of Ref. [12]. The "eDIS" band is a combination of the SLAC E122 [8, 9] and the JLab PVDIS [10, 11] experiments. Also indicated are the expected uncertainties from the planned P2 experiment [13] at Mainz, centered at the SM value.

elastic scattering off protons [6, 7]. The additional information entering Fig. 2 has been extracted from the parity-violating DIS experiments at SLAC [8, 9], as well as at JLab in the 6 GeV era [10, 11].

In contrast to the g_{AV}^{eq} and g_{VA}^{eq} , direct measurement on the g_{AA}^{eq} does not yet exist. So far, there is only experimental information from CERN [15] on their muonic counterparts, obtained by means of comparing the DIS cross section of positively charged left-handed muons directed on a carbon target with that of negatively charged right-handed ones. Neglecting radiative effects, their results can be written as

$$2g_{AA}^{\mu u} - g_{AA}^{\mu d} + 0.81(2g_{VA}^{\mu u} - g_{VA}^{\mu d}) = 1.45 \pm 0.41, \quad (6)$$

$$2g_{AA}^{\mu u} - g_{AA}^{\mu d} + 0.66(2g_{VA}^{\mu u} - g_{VA}^{\mu d}) = 1.70 \pm 0.79, \quad (7)$$

for the two beam energies $E_\mu = 200$ GeV and 120 GeV, and may be compared to the SM tree level predictions of 1.42 and 1.44, respectively. Note, that these results were previously summarized in Ref. [16] but the calculations are updated here using $\alpha^{-1} = 129$ and $\alpha^{-1} = 130$ for the inverse of the electromagnetic coupling at the two energies.

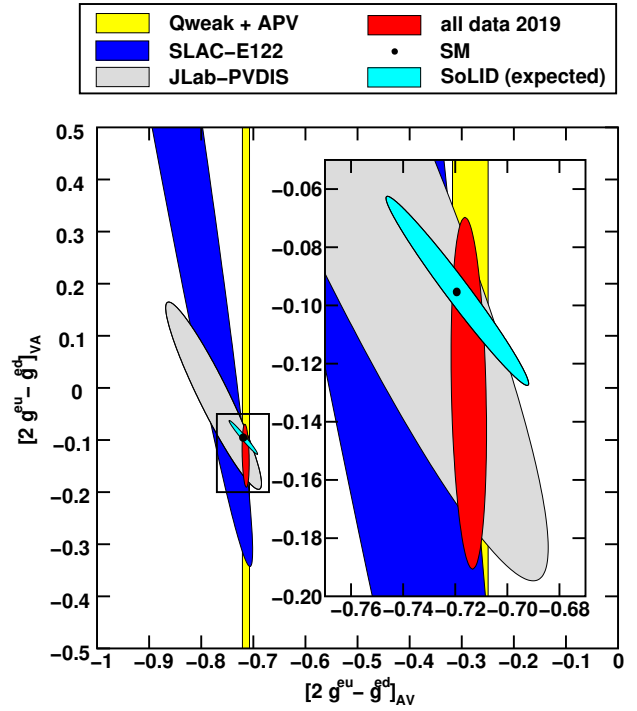


Fig. 2 Current experimental knowledge of the couplings g_{VA}^{eq} in the combinations given by the electric charge ratio of up and down quarks. The latest measurement is from the PVDIS experiment [10, 11] at JLab. Also indicated are the expected uncertainties from the planned SoLID project [14] at JLab, centered at the SM value.

With the SM value for $2g_{VA}^{\mu u} - g_{VA}^{\mu d} = -0.0954$, which is in good agreement with the PVDIS measurement [10, 11], we find the constraint,

$$2g_{AA}^{\mu u} - g_{AA}^{\mu d} = 1.57 \pm 0.38, \quad (8)$$

where we assumed that the (smaller) systematic error of the 200 GeV data was common to both beam energies. Assuming lepton universality, one may compare the error in Eq. (8) with the uncertainties shown in Fig. 1 and Fig. 2. But we stress that there is so far no direct measurement of the g_{AA}^{eq} for electron-quark interactions.

Neutral-Current Asymmetries in Lepton Scattering

The electroweak neutral-current induces various kinds of non-vanishing asymmetries for lepton and anti-lepton scattering, such as,

$$A_{ij}^{e^+e^-} \equiv \frac{\sigma_i^{e^+} - \sigma_j^{e^-}}{\sigma_i^{e^+} + \sigma_j^{e^-}}, \quad A_{RL}^{e^\pm} \equiv \frac{\sigma_R^{e^\pm} - \sigma_L^{e^\pm}}{\sigma_R^{e^\pm} + \sigma_L^{e^\pm}}, \quad (9)$$

with $i, j = R, L$, and analogous asymmetries for the heavier charged leptons. These are related to the asymmetries appearing in Ref. [17] by,

$$A_{\pm} = -A_{RL}^{\pm}, \quad C_i = A_{ii}^{e^+e^-}, \quad (10)$$

$$B_+ = A_{RL}^{e^+e^-}, \quad B_- = A_{LR}^{e^+e^-}. \quad (11)$$

Additionally, for unpolarized beams one can define,

$$A^{e^+e^-} \equiv \frac{\sigma^{e^+} - \sigma^{e^-}}{\sigma^{e^+} + \sigma^{e^-}}, \quad (12)$$

which is related to $A_{RL}^{e^+e^-}$, see Ref. [18].

$A_{RL}^{e^-}$ was first measured at SLAC [8, 9] in DIS, and then more precisely at JLab [10, 11], while $A_{LR}^{u\mu^-}$ is the aforementioned asymmetry as measured at CERN. Note that experiments targeting $A^{e^+e^-}$ have a great advantage for the positron beam being considered at JLab [19], in that much higher luminosities are achievable when polarization is not required. We provide explicit derivations of the asymmetries in Eqs. (9) in the appendix.

We now focus on asymmetries between positron and electron scattering, ignoring for simplicity nuclear and higher-order corrections. Considering the four quark flavors u, d, c, s and assuming symmetric charm and strange seas, $c = \bar{c}$ and $s = \bar{s}$, we have for isoscalar targets such as the deuteron,

$$A_{RL,d}^{e^+e^-} = \frac{3G_F Q^2}{2\sqrt{2}\pi\alpha} Y(y) \frac{R_V}{5 + 4R_C + R_S} \times \left[|\lambda| (2g_{VA}^{eu} - g_{VA}^{ed}) - (2g_{AA}^{eu} - g_{AA}^{ed}) \right], \quad (13)$$

where $|\lambda|$ is the magnitude of the beam polarization. $Q^2 \equiv -q^2$ with q the 4-momentum transfer from the beam to the target, and y is the fractional energy transfer. In terms of parton distribution functions (PDFs) with their dependence on Bjorken x and Q^2 implicit, and abbreviating $q^+ \equiv q + \bar{q}$ and $q_V \equiv q - \bar{q}$, one has,

$$Y(y) \equiv \frac{1 - (1-y)^2}{1 + (1-y)^2}, \quad R_V \equiv \frac{u_V + d_V}{u^+ + d^+}, \quad (14)$$

$$R_C \equiv \frac{2(c + \bar{c})}{u^+ + d^+}, \quad R_S \equiv \frac{2(s + \bar{s})}{u^+ + d^+}, \quad (15)$$

and similarly,

$$A_{RR,d}^{e^+e^-} = \frac{3G_F Q^2}{2\sqrt{2}\pi\alpha(5 + 4R_C + R_S)} \left\{ -|\lambda| [2(1 + R_C)g_{AV}^{eu} - (1 + R_S)g_{AV}^{ed}] - Y(y)R_V(2g_{AA}^{eu} - g_{AA}^{ed}) \right\}. \quad (16)$$

The expressions (13) and (16) can also be applied to $A_{LR,d}^{e^+e^-}$ and $A_{LL,d}^{e^+e^-}$, respectively, provided that the sign $|\lambda| \rightarrow -|\lambda|$ is flipped.

For unpolarized beams, $|\lambda| = 0$, Eq. (13) and (16) obviously simplify,

$$A_d^{e^+e^-} = -\frac{3G_F Q^2}{2\sqrt{2}\pi\alpha} Y(y) \frac{R_V (2g_{AA}^{eu} - g_{AA}^{ed})}{5 + 4R_C + R_S} = -1.06 \times 10^{-4} Q^2 \frac{Y(y)R_V(2g_{AA}^{eu} - g_{AA}^{ed})}{1 + 0.8R_C + 0.2R_S}, \quad (17)$$

where Q^2 is in GeV^2 , and where in the second line we assumed $\alpha^{-1} = 134$. From Eq. (17) one can see that the first generation g_{AA}^{eq} can be measured directly by comparing e^- and e^+ DIS cross sections, ideally with a high-intensity positron beam. Furthermore, to isolate the g_{AA}^{eq} an unpolarized beam is both necessary and sufficient. This asymmetry is comparable in size to the PVDIS asymmetry that has been measured at JLab to (2-3)% precision [10, 11]. We note that unlike the PVDIS asymmetry where the contribution from the $2g_{VA}^{eu} - g_{VA}^{ed}$ is quite small, the asymmetry in Eq. (17) arises fully from the couplings we wish to measure.

In practice, such a measurement will encounter both experimental and theoretical challenges. The DIS cross section difference between e^- and e^+ scattering is subject to higher-order QED corrections. Box graphs describing two photon and photon- Z boson exchange have to be included, combined with real photon radiation to render the result infrared finite. The expected size of these corrections is $\mathcal{O}(\alpha/\pi)$, *i.e.* at the 10^{-3} level, and without a logarithmic enhancement. The separation of the weak couplings g_{AA}^{eq} requires theory predictions of such higher-order effects at the level of 1% or better. Theory techniques are ready to achieve this goal at the parton level including two-loop Feynman diagrams. A parton-level calculation is expected to be valid at large Q^2 , but additional investigations will be required to improve our understanding of related uncertainties in the transition region towards the Q^2 values of JLab. It is beyond the scope of this article to perform a detailed study of these corrections. We trust that with dedicated efforts, future theory work will allow to control the associated uncertainties at the required level.

Feasibility of $A_d^{e^+e^-}$ Measurement at JLab

We now consider to expose the planned Solenoid Large Intensity Device (SoLID) [14] to a possible 11 GeV positron beam from the Continuous Electron Beam Accelerator Facility (CEBAF) at JLab in order to measure $A_d^{e^+e^-}$ on a deuteron target. SoLID is a general-purpose, large-acceptance spectrometer that can handle the high luminosities of CEBAF. It is currently being planned for the experimental Hall A for measurements of PVDIS, semi-inclusive DIS (SIDIS), and other

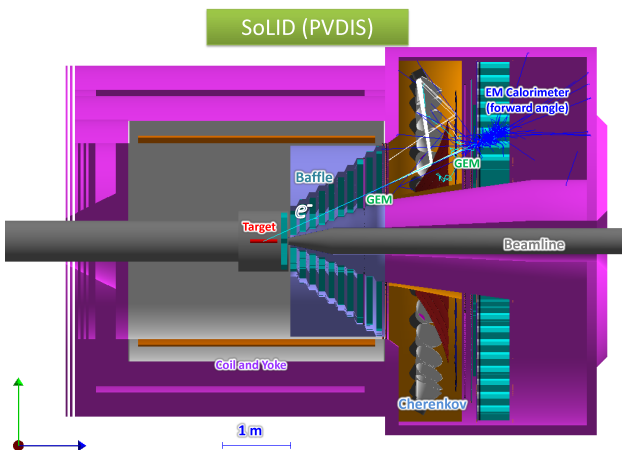


Fig. 3 SoLID in its PVDIS configuration. The electron (or positron) beam enters from the left and incident on a 40-cm long liquid target. Scattered electrons are detected by GEM chambers, a gas Cherenkov detector, and an electromagnetic calorimeter. A set of "baffles" (slitted shielding) can be used at high luminosity to reduce backgrounds, but may not be needed for the positron running discussed here.

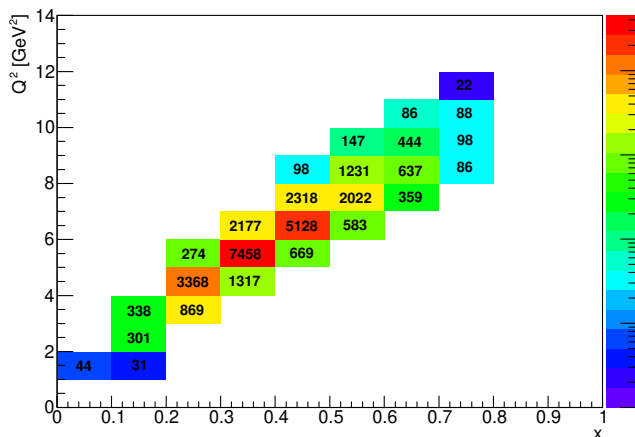


Fig. 4 Generated rates (in Hz) assuming the SoLID PVDIS configuration with a 40 cm long liquid deuterium target exposed to a $3 \mu\text{A}$ beam current, shown on a (x, Q^2) grid (Q^2 in GeV^2). The cut on the invariant mass of the hadronic final state system of $W > 2 \text{ GeV}$ and the $Q^2 > 1 \text{ GeV}^2$ cut have been applied to ensure DIS. Baffles are not assumed.

physics processes including J/ψ production and Deeply Virtual Compton Scattering (DVCS). The most suitable setup for our $A_d^{e^+e^-}$ measurement will be SoLID's PVDIS configuration shown in Fig. 3. To use the PVDIS setup for positron scattering, the polarity of the solenoid magnet will be reversed such that the acceptance of the scattered positrons can be kept as close to that of electrons as possible. Because of the large acceptance of SoLID, it is possible to measure $A_d^{e^+e^-}$ over a wide kinematic range and use the kinematic dependence of the asymmetry to isolate the electroweak contribution due to the g_{AA}^{eq} from other competing effects.

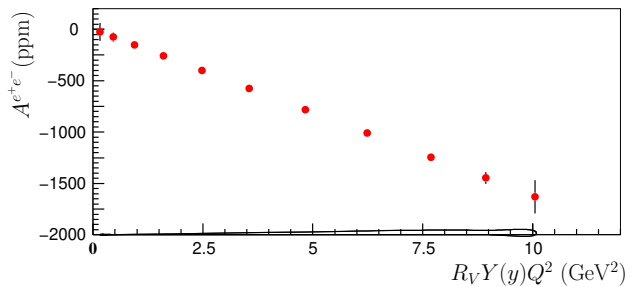


Fig. 5 Expected value and statistical uncertainty (in ppm) for a measurement of $A_d^{e^+e^-}$ using 20 days of $3 \mu\text{A}$ unpolarized beam at 100% efficiency directed at a 40 cm long liquid deuterium target, interchanging between positrons and electrons. SoLID is assumed in its PVDIS configuration without baffles. The horizontal band at -2000 ppm shows the total PDF uncertainty (see main text for details), multiplied by a factor of 10 for better visibility.

We studied the feasibility of a measurement of the asymmetry $A_d^{e^+e^-}$ using the simulated DIS rates from the SoLID pre-Conceptual Design Report [20] for a $3 \mu\text{A}$ positron beam incident on a 40 cm liquid deuterium target, as detailed in Fig. 4. The value $3 \mu\text{A}$ for the beam current was chosen based on the present expectation of the positron source, demonstrated by the PEPPo (Polarized Electrons for Polarized Positrons) experiment [19]. The statistical uncertainty estimate assumes 20 days of beam time at 100% efficiency as shown in Fig. 5. We assumed that SoLID will be used in its PVDIS configuration with the baffles removed. If baffles were used, the required beam time would be about three times as long. The size of the asymmetry at each Q^2 point was calculated from Eq. (17), and both MMHT2014 [21] (NLO120 grid) and CT18 [22] (CT18NLO grid) PDFs averaged over the corresponding x range. To estimate the total PDF uncertainty in the asymmetry calculation, we took the average of the $A_d^{e^+e^-}$ results from the two PDF sets as central values, and the half-differences between the two was added in quadrature to the uncertainty calculated using the PDF eigenvector sets. This total PDF uncertainty varies from 10 ppm to below 1 ppm.

The binned asymmetries can be fitted using

$$A_d^{e^+e^-}(Q^2) = a + bR_V \left[\frac{1 - (1 - y)^2}{1 + (1 - y)^2} \right] Q^2, \quad (18)$$

where a and b are free parameters. We found the variation $\Delta b = \pm 2.75 \text{ ppm}$, resulting in a combined statistical plus PDF uncertainty of $\Delta(2g_{AA}^{eu} - g_{AA}^{ed}) = \pm 0.026$. For an actual measurement, the fitting function (18) can be modified to account for other contributions, such as QED corrections, and differences in beam intensities and energies, and other experimental effects between e^+ and e^- runs. Depending on the size of these experimental effects, the systematic uncertainty may dominate.

These estimates demonstrate that a measurement of the g_{AA}^{eq} is possible using SoLID, provided one can switch between a positron and an electron beam. The differences between the e^+ and e^- beams, from intensity, energy, position, direction, and spot size, need to be kept as small as possible and the effects studied carefully. One must also require that the difference in spectrometer response to electrons and positrons is below the statistical error, or can be corrected for. Note that while these requirements may look daunting to reach in practice, they had been achieved in the 96-day long CERN experiment [15], where a switch between μ^+ and μ^- took place twice in each 12-day run period. Care was taken to ensure that the μ^\pm data were collected at the same intensity such that many systematic effects cancel, and the spectrometer magnet was operating at full saturation so that the field could be reproduced to high precision with each polarity reversal, while a 40 meter long carbon target assured the required rates.

New Physics Mass Limit

The energy scale, Λ , up to which new physics Beyond the SM (BSM) is testable, can be quantified in terms of perturbations of the SM Lagrangian (1), that is by replacements of the form,

$$\frac{G_F}{\sqrt{2}}g_{ij} \rightarrow \frac{G_F}{\sqrt{2}}g_{ij} + \eta_{ij}^q \frac{4\pi}{(\Lambda_{ij}^q)^2}, \quad (19)$$

where $ij = AV, VA, AA$ and we assumed that the new physics is strongly coupled with a coupling g given by $g^2 = 4\pi$. Without the specification of a particular BSM scenario, any combination of the g_{AA}^{eq} can be modified, both with constructive or destructive interference with the SM, *i.e.* $\eta_{ij}^q = \pm 1$. Therefore, a determination of the combination $2g_{AA}^{eu} - g_{AA}^{ed}$ through $A_d^{e^+e^-}$ puts constraints on Λ_{AA}^u and Λ_{AA}^d . Of course, the sensitivity of a measurement of $2g_{AA}^{eu} - g_{AA}^{ed}$ is reduced (enhanced) in models in which the contributions to g_{AA}^{eu} and g_{AA}^{ed} are (anti-)correlated. In general, any BSM model will produce a shift in the combination $\cos \alpha g_{AA}^{eu} + \sin \alpha g_{AA}^{ed}$ for some value of α , to which a measurement of $2g_{AA}^{eu} - g_{AA}^{ed}$ has maximal (minimal) sensitivity for $\tan \alpha = -1/2$ (+2). The associated new physics scales which can be probed given a total uncertainty $\Delta(\cos \alpha g_{AA}^{eu} + \sin \alpha g_{AA}^{ed})$, are given by,

$$\Lambda(\alpha) = v \sqrt{\frac{8\pi}{\Delta(\cos \alpha g_{AA}^{eu} + \sin \alpha g_{AA}^{ed})}}, \quad (20)$$

where $v = (\sqrt{2}G_F)^{-1/2} = 246.22$ GeV is the Higgs vacuum expectation value setting the electroweak scale. Thus, in models predicting $\Delta g_{AA}^{eu} = 0$ ($\alpha = \pi/2$) or

$\Delta g_{AA}^{ed} = 0$ ($\alpha = 0$) a constraint $\Delta(2g_{AA}^{eu} - g_{AA}^{ed}) = \pm 0.03$, can probe Λ_{AA}^d up to 7.1 TeV or Λ_{AA}^u up to 10.1 TeV, respectively. The maximal 1σ -sensitivity is given by $\alpha = \arctan(-1/2)$ and

$$\Lambda = v \sqrt{\frac{8\sqrt{5}\pi}{\Delta(2g_{AA}^{eu} - g_{AA}^{ed})}} = 10.7 \text{ TeV}, \quad (21)$$

while the minimum $\Lambda = 0$ is given by $\alpha = \arctan(2)$.

Any model predicting a significant effect in the g_{AA}^{eq} , while leaving the $g_{AV,VA}^{eq}$ unaltered, is presumably contrived or tuned; however, the g_{AA}^{eq} are couplings independent of the $g_{AV,VA}^{eq}$, and their constraints on BSM physics are complementary. Conversely, if new physics is seen in the $g_{AV,VA}^{eq}$, it would be of paramount importance to measure the g_{AA}^{eq} , as well.

Summary

We reviewed the current knowledge on the electron-quark effective couplings g_{AV}^{eq} , g_{VA}^{eq} and g_{AA}^{eq} , all of which are accessible in charged lepton scattering. The g_{AA}^{eq} can be extracted from $A_d^{e^+e^-}$, the DIS cross section asymmetry between a positron and an electron beam scattering off a deuterium target, assuming that other contributions can be reliably separated and that all experimental systematic uncertainties are under control. An exploratory calculation was performed to study the possibility of measuring $A_d^{e^+e^-}$ by exposing the planned SoLID spectrometer at JLab to a future unpolarized positron beam. Our results are encouraging, mapping out the path to the first measurement of the electron-quark g_{AA}^{eq} within a reasonable amount of beam time. A targeted precision of $\Delta(2g_{AA}^{eu} - g_{AA}^{ed}) = \pm 0.03$ would provide an order of magnitude stronger constraint compared to the one on the muonic $g_{AA}^{\mu q}$ from CERN. Detailed studies are underway on the control of experimental systematic uncertainties and QED corrections.

Acknowledgements X.Z. was supported by the U.S. Department of Energy (DOE) Early Career Award SC00-03885 during the early stage of this work, and currently by the U.S. DOE under Award number DE-SC0014434. The work of J.E. and H.S. is supported by the German-Mexican research collaboration grant SP 778/4-1 (DFG) and 278017 (CONACyT).

Appendix A: Neutral-current DIS asymmetries

In this appendix, we derive asymmetries of lepton deep inelastic scattering off a nuclear target arising from the interference between electromagnetic and weak neutral current (NC) interactions. We are interested in the case of relatively small momentum transfer.

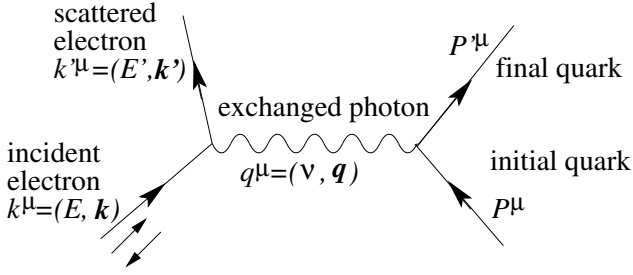


Fig. 6 One-photon exchange in electron-quark DIS. For the weak neutral current interaction, the photon is replaced by a Z boson.

Neutral-current weak interaction Lagrangian

The kinematics of lepton-quark scattering is illustrated in Fig. 6, where the photon-fermion vertex is given by $-ie\gamma^\mu Q_f$ with Q_f the fermion electric charge in units of $e = \sqrt{4\pi\alpha}$. Likewise, the Z -fermion vertex reads,

$$-i\frac{g}{2\cos\theta_W}\gamma^\mu (g_V^f - g_A^f\gamma^5), \quad (\text{A.1})$$

The matrix element for NC eq scattering can now be written,

$$\frac{1}{i}\mathcal{M}_{NC} = \bar{l}_f \left[-i\frac{g}{2\cos\theta_W}\gamma^\mu (g_V^l - g_A^l\gamma^5) \right] l_i \quad (\text{A.2})$$

$$\left(-i\frac{g_{\mu\nu} - \frac{q_\mu q_\nu}{M_Z^2}}{q^2 - M_Z^2} \right) \bar{q}_f \left[-i\frac{g}{2\cos\theta_W}\gamma^\nu (g_V^q - g_A^q\gamma^5) \right] q_i,$$

where M_Z is the Z boson mass, and $l_{i,f}$ and $q_{i,f}$ are the Dirac spinors for the initial and final state electrons and quarks, respectively. At the SM tree level, the gauge coupling g is related to G_F ,

$$\frac{G_F}{\sqrt{2}} = \frac{g^2}{8M_Z^2\cos^2\theta_W}, \quad (\text{A.3})$$

so that for small momentum transfer, $|q^2| \ll M_Z^2$, and dropping the vector-vector interactions, the amplitude in Eq. (A.2) derives from the neutral-current weak interaction Lagrangian

$$\mathcal{L}_{int}^{NC} = \frac{G_F}{\sqrt{2}} [g_{VV}^{eq} \bar{l}_f \gamma^\mu l_i \bar{q}_f \gamma_\mu q_i$$

$$+ g_{VA}^{eq} \bar{l}_f \gamma^\mu l_i \bar{q}_f \gamma_\mu \gamma^5 q_i + g_{AV}^{eq} \bar{l}_f \gamma^\mu \gamma^5 l_i \bar{q}_f \gamma_\mu q_i$$

$$+ g_{AA}^{eq} \bar{l}_f \gamma^\mu \gamma^5 l_i \bar{q}_f \gamma_\mu \gamma^5 q_i], \quad (\text{A.4})$$

where we used the same symbols for Dirac spinor fields and coefficient functions.

One-photon exchange amplitude and Z - γ^* interference

For incoming leptons with helicity h (the case of anti-leptons will be treated separately), we have the one-photon exchange amplitude,

$$\mathcal{M}_\gamma^h = -Q_l Q_q \frac{4\pi\alpha}{q^2} (\bar{l}_f \gamma^\mu P_h l_i) (\bar{q}_f \gamma_\mu q_i), \quad (\text{A.5})$$

where,

$$P_h \equiv \frac{1 + h\gamma^5}{2}, \quad (\text{A.6})$$

is the projection operator for right-handed ($h = +1$) and left-handed ($h = -1$) leptons. The cross section of the electromagnetic process is,

$$\sum_{\text{spins}} |\mathcal{M}_h^\gamma|^2 = 16Q_l^2 Q_q^2 \left(\frac{4\pi\alpha}{q^2} \right)^2$$

$$\times [(Pk)(P'k') + (P'k')(P'k)]. \quad (\text{A.7})$$

For the weak neutral current interaction we have,

$$\mathcal{M}_{NC}^h = \sqrt{2}G_F [\bar{l}_f \gamma^\mu (g_V^l - g_A^l\gamma^5) P_h l_i]$$

$$\times [\bar{q}_f \gamma_\mu (g_V^q - g_A^q\gamma^5) q_i], \quad (\text{A.8})$$

so that the interference term is given by,

$$(\mathcal{M}_\gamma^h)^* \mathcal{M}_{NC}^h = -\frac{4\sqrt{2}\pi G_F \alpha}{q^2} Q_l Q_q (\bar{l}_i P_{-h} \gamma^\mu l_f) \times (\text{A.9})$$

$$[\bar{l}_f \gamma^\nu (g_V^l - g_A^l\gamma^5) P_h l_i] (\bar{q}_i \gamma_\mu q_f) [\bar{q}_f \gamma_\nu (g_V^q - g_A^q\gamma^5) q_i].$$

Averaging over initial and summing over the final spin states,

$$\sum_{\text{spins}} (\mathcal{M}_\gamma^h)^* \mathcal{M}_{NC}^h = -\frac{64\sqrt{2}\pi G_F \alpha}{q^2} Q_l Q_q \times \quad (\text{A.10})$$

$$\{ (kP)(k'P') [g_V^l g_V^q - h g_A^l g_V^q - h g_V^l g_A^q + g_A^l g_A^q] +$$

$$(k'P')(kP) [g_V^l g_V^q - h g_A^l g_V^q + h g_V^l g_A^q - g_A^l g_A^q] \}.$$

Likewise, denoting the anti-lepton coefficient functions by $v_{i,f}$, for incoming anti-leptons with helicity h the leptonic currents in Eq. (A.5) and (A.8) are now $(\bar{v}_i P_h \gamma^\mu v_f)$ and $[\bar{v}_i P_h \gamma^\mu (g_V^l - g_A^l\gamma^5) v_f]$, respectively. Eq. (A.10) then also applies for anti-leptons as long as one substitutes $h \rightarrow -h$ and $g_A^q \rightarrow -g_A^q$.

For anti-quarks at the γ or Z^0 vertex one substitutes analogously the quark-coefficient functions by those of anti-quarks, with the result that Eq. (A.10) applies when one replaces $g_A^q \rightarrow -g_A^q$ in the case of lepton scattering. Finally, for anti-lepton scattering off anti-quarks one needs to substitute $h \rightarrow -h$ in Eq. (A.10).

Electroweak neutral current cross section asymmetries

In DIS one has to combine the scattering cross sections for all quarks in the target with weights according to the PDFs. From the definition in Eq. (9) we have,

$$A_{RL}^{e^\pm} = \frac{|\mathcal{M}_Z + \mathcal{M}_\gamma|_{h=+|\lambda|}^2 - |\mathcal{M}_Z + \mathcal{M}_\gamma|_{h=-|\lambda|}^2}{|\mathcal{M}_Z + \mathcal{M}_\gamma|_{h=+|\lambda|}^2 + |\mathcal{M}_Z + \mathcal{M}_\gamma|_{h=-|\lambda|}^2}$$

$$\approx \frac{(\mathcal{M}_\gamma^* \mathcal{M}_Z)_{h=+|\lambda|} - (\mathcal{M}_\gamma^* \mathcal{M}_Z)_{h=-|\lambda|}}{|\mathcal{M}_\gamma|^2}. \quad (\text{A.11})$$

If we now use the previous results, inserting the Mandelstam variables neglecting lepton and quark masses, *i.e.*, $s \equiv (k + P)^2 = 2kP = 2k'P'$ with $P_{\text{quark}} = xP_{\text{nucleon}}$, and likewise $u \equiv (k - P')^2 = -2kP' = -2k'P = -(1 - y)s$,

$$A_{RL}^{e^-} = |\lambda| \frac{G_F Q^2}{2\sqrt{2}\pi\alpha} \left\{ \frac{\sum q(x, Q^2) Q_q g_{AV}^{eq} [1 + (1 - y)^2]}{\sum q(x, Q^2) Q_q^2 [1 + (1 - y)^2]} + \frac{\sum q(x, Q^2) Q_q g_{VA}^{eq} [1 - (1 - y)^2]}{\sum q(x, Q^2) Q_q^2 [1 + (1 - y)^2]} \right\}, \quad (\text{A.12})$$

where λ is the beam polarization and $q(x, Q^2)$ are PDFs. The value $Q_l = -1$ for electron scattering, $Q^2 \equiv -q^2$, and the definitions of g_{AV}^{eq} and g_{VA}^{eq} were also used. We note that for the antiquark contributions the couplings g_A^q (and therefore all g_{VA}^{eq}) appear with an extra minus sign. For a proton target we obtain,

$$A_{RL,p}^{e^-} = |\lambda| \frac{3G_F Q^2}{2\sqrt{2}\pi\alpha(4U^+ + D^+)} [(2U^+ g_{AV}^{eu} - D^+ g_{AV}^{ed}) + Y(2u_V g_{VA}^{eu} - d_V g_{VA}^{ed})], \quad (\text{A.13})$$

where we have further abbreviated $U^+ \equiv u^+ + c^+$ and $D^+ \equiv d^+ + s^+$, and have assumed $c = \bar{c}$ and $s = \bar{s}$ (and thus $c_V = s_V = 0$). The function Y is defined in Eq. (14) and we will omit its dependence on y hereafter. For deuterium or other isoscalar targets (ignoring nuclear effects), we substitute $u \rightarrow u + d$ and $d \rightarrow u + d$ in the expression for $A_{RL,p}^{e^-}$ above, and assume that c and s are the same in the proton and the neutron:

$$A_{RL,d}^{e^-} = |\lambda| \frac{3G_F Q^2}{2\sqrt{2}\pi\alpha(5 + 4R_C + R_S)} \{ [2(1 + R_C) g_{AV}^{eu} - (1 + R_S) g_{AV}^{ed}] + Y(2g_{VA}^{eu} - g_{VA}^{ed}) R_V \}. \quad (\text{A.14})$$

Ignoring the heavier s and c quarks, these expressions simplify further,

$$A_{RL,p}^{e^-} \approx |\lambda| \frac{3G_F Q^2}{2\sqrt{2}\pi\alpha(4u^+ + d^+)} [(2u^+ g_{AV}^{eu} - d^+ g_{AV}^{ed}) + Y(2u_V g_{VA}^{eu} - d_V g_{VA}^{ed})], \quad (\text{A.15})$$

$$A_{RL,d}^{e^-} \approx |\lambda| \frac{3G_F Q^2}{10\sqrt{2}\pi\alpha} [(2g_{AV}^{eu} - g_{AV}^{ed}) + R_V Y(2g_{VA}^{eu} - g_{VA}^{ed})]. \quad (\text{A.16})$$

We now turn to the calculation of $A_{RL}^{e^+e^-}$,

$$A_{RL}^{e^+e^-} = \frac{|\mathcal{M}_Z^{e^+} + \mathcal{M}_\gamma^{e^+}|_{h=+|\lambda|}^2 - |\mathcal{M}_Z^{e^-} + \mathcal{M}_\gamma^{e^-}|_{h=-|\lambda|}^2}{|\mathcal{M}_Z^{e^+} + \mathcal{M}_\gamma^{e^+}|_{h=+|\lambda|}^2 + |\mathcal{M}_Z^{e^-} + \mathcal{M}_\gamma^{e^-}|_{h=-|\lambda|}^2} \approx \frac{(\mathcal{M}_\gamma^{e^+} \mathcal{M}_Z^{e^+})_{+|\lambda|} - (\mathcal{M}_\gamma^{e^-} \mathcal{M}_Z^{e^-})_{-|\lambda|}}{|\mathcal{M}_\gamma|^2}, \quad (\text{A.17})$$

where the approximation is valid for $Q^2 \ll M_Z^2$. For a nuclear target,

$$A_{RL}^{e^+e^-} = \frac{G_F Q^2 Y \sum_q q_V Q_q (|\lambda| g_{VA}^{eq} - g_{AA}^{eq})}{2\sqrt{2}\pi\alpha \sum_q q^+ Q_q^2}. \quad (\text{A.18})$$

and likewise,

$$A_{RR}^{e^+e^-} = \frac{G_F Q^2 \sum_q Q_q [-|\lambda| q^+ g_{AV}^{eq} - q_V Y g_{AA}^{eq}]}{2\sqrt{2}\pi\alpha \sum_q q^+ Q_q^2}. \quad (\text{A.19})$$

By substituting $|\lambda| \rightarrow -|\lambda|$ one can obtain $A_{LR}^{e^+e^-}$ from Eq. (A.18), and $A_{LL}^{e^+e^-}$ from Eq. (A.19). For $A_{e^+e^-}$ one can use (A.18) or (A.19) and set $|\lambda| = 0$. For the proton,

$$A_{RL,p}^{e^+e^-} = \frac{3G_F Q^2 Y}{2\sqrt{2}\pi\alpha(4U^+ + D^+)} [|\lambda|(2u_V g_{VA}^{eu} - d_V g_{VA}^{ed}) - (2u_V g_{AA}^{eu} - d_V g_{AA}^{ed})], \quad (\text{A.20})$$

$$A_{RR,p}^{e^+e^-} = \frac{3G_F Q^2}{2\sqrt{2}\pi\alpha(4U^+ + D^+)} [-|\lambda|(2U^+ g_{AV}^{eu} - D^+ g_{AV}^{ed}) - Y(2u_V g_{AA}^{eu} - d_V g_{AA}^{ed})], \quad (\text{A.21})$$

and for the deuteron,

$$A_{RL,d}^{e^+e^-} = \frac{3G_F Q^2 Y R_V}{2\sqrt{2}\pi\alpha(5 + 4R_C + R_S)} [|\lambda|(2g_{VA}^{eu} - g_{VA}^{ed}) - (2g_{AA}^{eu} - g_{AA}^{ed})], \quad (\text{A.22})$$

$$A_{RR,d}^{e^+e^-} = \frac{3G_F Q^2}{2\sqrt{2}\pi\alpha(5 + 4R_C + R_S)} \{ -|\lambda|[2(1 + R_C) g_{AV}^{eu} - (1 + R_S) g_{AV}^{ed}] - Y R_V(2g_{AA}^{eu} - g_{AA}^{ed}) \}. \quad (\text{A.23})$$

Finally, if only u and d quarks are included,

$$A_{RL,p}^{e^+e^-} \approx \frac{3G_F Q^2 Y}{2\sqrt{2}\pi\alpha(4u^+ + d^+)} [|\lambda|(2u_V g_{VA}^{eu} - d_V g_{VA}^{ed}) - (2u_V g_{AA}^{eu} - d_V g_{AA}^{ed})], \quad (\text{A.24})$$

$$A_{RR,p}^{e^+e^-} \approx \frac{3G_F Q^2}{2\sqrt{2}\pi\alpha(4u^+ + d^+)} [-|\lambda|(2u^+ g_{AV}^{eu} - d^+ g_{AV}^{ed}) - (2u_V g_{AA}^{eu} - d_V g_{AA}^{ed}) Y], \quad (\text{A.25})$$

and

$$A_{RL,d}^{e^+e^-} \approx \frac{3G_F Q^2 Y R_V}{10\sqrt{2}\pi\alpha} [|\lambda|(2g_{VA}^{eu} - g_{VA}^{ed}) - (2g_{AA}^{eu} - g_{AA}^{ed})]. \quad (\text{A.26})$$

$$A_{RR,d}^{e^+e^-} \approx \frac{3G_F Q^2}{10\sqrt{2}\pi\alpha} [-|\lambda|(2g_{AV}^{eu} - g_{AV}^{ed}) - Y R_V(2g_{AA}^{eu} - g_{AA}^{ed})]. \quad (\text{A.27})$$

The asymmetry measured at CERN on ^{12}C was,

$$A_{LR,C}^{\mu^+\mu^-} = -\frac{3G_F Q^2 Y R_V}{2\sqrt{2}\pi\alpha(5 + 4R_C + R_S)} \left[(2g_{AA}^{\mu u} - g_{AA}^{\mu d}) + |\lambda|(2g_{VA}^{\mu u} - g_{VA}^{\mu d}) \right], \quad (\text{A.28})$$

while for SoLID we can use unpolarized beams to allow for higher intensities and measure on the deuteron,

$$A_d^{e^+e^-} = -\frac{3G_F Q^2 Y R_V (2g_{AA}^{eu} - g_{AA}^{ed})}{2\sqrt{2}\pi\alpha (5 + 4R_C + R_S)}. \quad (\text{A.29})$$

References

1. P. A. Zyla *et al.* (Particle Data Group), *Prog. Theor. Exp. Phys.* **2020**, 083C01 (2020) doi:10.1093/ptep/ptaa104
2. J. Erler and S. Su, *Prog. Part. Nucl. Phys.* **71**, 119 (2013) doi:10.1016/j.ppnp.2013.03.004 arXiv:1303.5522 [hep-ph]
3. J. Erler, C. J. Horowitz, S. Mantry and P. Souder, *Ann. Rev. Nucl. Part. Sci.* **64**, 269 (2014) doi:10.1146/annurev-nucl-102313-025520 arXiv:1401.6199 [hep-ph]
4. C. S. Wood *et al.*, *Science* **275**, 1759 (1997) doi:10.1126/science.275.5307.1759
5. J. Guena, M. Lintz and M. A. Bouchiat, *Mod. Phys. Lett. A* **20**, 375 (2005) doi:10.1142/S0217732305016853 arXiv:physics/0503143 [physics]
6. D. Androić *et al.* (Qweak Collaboration), *Phys. Rev. Lett.* **111**, 141803 (2013) doi:10.1103/PhysRevLett.111.141803 arXiv:1307.5275 [nucl-ex]
7. D. Androić *et al.* (Qweak Collaboration), *Nature* **557**, 207 (2018) doi:10.1038/s41586-018-0096-0 arXiv:1905.08283 [nucl-ex]
8. C. Y. Prescott *et al.*, *Phys. Lett. B* **77**, 347 (1978) doi:10.1016/0370-2693(78)90722-0
9. C. Y. Prescott *et al.*, *Phys. Lett. B* **84**, 524 (1979) doi:10.1016/0370-2693(79)91253-X
10. D. Wang *et al.* (PVDIS Collaboration), *Nature* **506**, 67 (2014) doi:10.1038/nature12964
11. D. Wang *et al.* (PVDIS Collaboration), *Phys. Rev. C* **91**, 045506 (2015) doi:10.1103/PhysRevC.91.045506 arXiv:1411.3200 [nucl-ex]
12. G. Toh *et al.*, *Phys. Rev. Lett.* **123**, 073002 (2019) doi:10.1103/PhysRevLett.123.073002 arXiv:1905.02768 [physics.atom-ph]
13. D. Becker *et al.* (P2 Collaboration), *Eur. Phys. J. A* **54**, 208 (2018) doi:10.1140/epja/i2018-12611-6 arXiv:1802.04759 [nucl-ex]
14. J. P. Chen *et al.* (SoLID Collaboration) arXiv:1409.7741 [nucl-ex]
15. A. Argento *et al.*, *Phys. Lett. B* **120**, 245 (1983) doi:10.1016/0370-2693(83)90665-2
16. J. Erler and M. J. Ramsey-Musolf, *Prog. Part. Nucl. Phys.* **54**, 351 (2005) doi:10.1016/j.ppnp.2004.08.001 arXiv:hep-ph/0404291 [hep-ph]
17. H. Spiesberger, preprint DESY-89-175
18. S. M. Berman and J. R. Primack, *Phys. Rev. D* **9**, 2171 (1974) doi:10.1103/PhysRevD.9.2171
19. L. S. Cardman, “The PEPPo method for polarized positrons and PEPPo II,” *AIP Conf. Proc.* **1970**, no.1, 050001 (2018) doi:10.1063/1.5040220
20. SoLID Collaboration (2019) <https://hallaweb.jlab.org/12GeV/SoLID/files/solid-precdr-Nov2019.pdf>
21. L. A. Harland-Lang, A. D. Martin, P. Motylinski and R. S. Thorne, *Eur. Phys. J. C* **75**, 204 (2015) doi:10.1140/epjc/s10052-015-3397-6 arXiv:1412.3989 [hep-ph]
22. T. J. Hou *et al.*, *Phys. Rev. D* **103**, 014013 (2021) doi:10.1103/PhysRevD.103.014013 arXiv:1912.10053 [hep-ph]